Advances in Nano Research, *Vol. 4, No. 3 (2016) 157-165*
DOI: http://dx.doi.org/10.12989/anr.2016.4.3.157

Controlled synthesis of mesoporous codoped titania nanoparticles and their photocatalytic activity

John E. Mathis*[1,2], Michelle K. Kidder[1], Yunchao Li[1], Jinshui Zhang[1] and M.P. Paranthaman[1]

[1]*Chemical Sciences Division, Oak Ridge National Laboratory, Oak Ridge, TN 37831, USA*
[2]*Physical Sciences Department, Embry-Riddle Aeronautical University, Daytona Beach, FL 32114, USA*

(Received January 23, 2016, Revised June 30, 2016, Accepted June 24, 2016)

Abstract. The photocatalytic (PC) activity of anatase titania nanoparticles can be improved through codoping with transition metals and nitrogen. In addition, the PC activity can also be improved by creating monodisperse, mesoporous nanoparticles of titania. The question naturally arose as to whether combining these two characteristics would result in further improvement in the PC activity or not. Herein, we describe the synthesis and photocatalytic characteristics of codoped, monodisperse anatase titania. The transition metals tested in the polydisperse and the monodisperse forms were Mn, Co, Ni, and Cu. In each case, it was found that the monodisperse version had a higher PC activity compared to the corresponding polydisperse version.

Keywords: titania; codoped; phototcatalysis; macro-spores; micro-spheres; hydrothermal method; hybrid method

1. Introduction

The poor conductivity of TiO_2 stands in the way of being more an efficient photocatalyst. In order for the photo-generated holes and electrons to be effective, they must reach the surface of the material before they recombine, the faster they can move, the less likely they will combine. Unfortunately, the electron mobility in TiO_2 is quite low, having a value of 0.1 cm^2/V.sec in mesoporous TiO_2 thin films (Tiwana *et al*. 2011). Using structures with nanometer-sized dimensions mitigate this somewhat by reducing the distance the charges through which the particles move, but on the other hand, the charges must then navigate across grain boundaries and particle interfaces. The higher the crystallinity of the material, the lower the barriers for the charges (Benko *et al*. 2003). It has also been shown that materials consisting of nano-sized beads of non-uniform size also suffer from poor charge mobility (Pascoe *et al*. 2014).

Adding metal ions to the TiO_2 structure through doping can increase conductivity. Among the metals used for doping TiO_2 that show significant increases in conductivity are Nb (Yamada *et al*. 2007, Liu *et al*. 2010, Wang *et al*. 2009), Sb (Wang *et al*. 2009), Ta (Wang *et al*. 2009), and Sn (Dorman *et al*. 2014). Doping with anions such as fluorine also increases conductivity *(*Seo *et al.*

*Corresponding author, Professor, E-mail: mathisjo@erau.edu

http://www.techno-press.com/?journal=anr&subpage=7 ISSN: 2287-237X (Print), 2287-2388 (Online)

2011). Codoping titania, which in the present study uses a combination of transition metals and nitrogen as dopants, can also increase conductivity and provide ionic stability. The combination of these dopants produces *n-p* co-doping of TiO_2, with increased stability of the ions within the lattice (Zhu *et al*. 2009). Not only does this n-p structure increase conductivity, but it also reduces the band gap of TiO_2. An experimental study (Li *et al*. 2011) found that chromium-, nitrogen-codoped TiO_2 (denoted as (Cr, N)TiO_2) exhibited promising photocatalytic properties as shown by the degradation of methylene blue in aqueous solutions. The optimal amount of Cr dopant was found to be 3 percent. A later study of hydrothermally-prepared (Cr, N)TiO_2 for use as an electrode in lithium-ion batteries reported increased conductivity (Bi *et al*. 2014).

Codoping does not affect the crystallinity of titania nanoparticles. Park and Kim (2005) determined that doping titania up to 15 percent with cobalt had no effect on the a-axis properties of rutile titania. Moreover, nitrogen doping has not been found to significantly alter the crystal structure (Thompson and Yates Jr. 2006), and, as will be shown in this report, codoping anatase titania with both transition metals and nitrogen shows identical XRD patterns.

A recent study (Mathis *et al*. 2013) compared the light-absorbing properties of mesoporous TiO_2 nanoparticles when they were co-doped with nitrogen and a sequence of the first-row transition metals, chromium, manganese, iron, cobalt, nickel, copper, and zinc. A hydrothermal process was used to synthesize the metal-doped TiO_2 mesoporous nanoparticles, which was followed by nitrogen doping of the nanoparticles by annealing them in a high-temperature furnace under flowing ammonia. Two levels of metal doping were used, 2.5 percent and 5.0 percent. The result was increased visible-light absorption for both levels, but the 2.5 percent level had much higher absorbance values.

A follow-up study was done on the photocatalytic (PC) activity of these co-doped nanoparticles (Mathis *et al*. 2016). The nanoparticles were suspended in a solution of methylene blue in isopropanol, and the degradation of the methylene blue solution, as it was exposed to the light from a xenon arc lamp, was monitored. Four of the metals used for codoping – manganese, iron, copper, and cobalt – exhibited PC activity greater than anatase titania doped with just nitrogen. (Mn,N)TiO_2 had the highest PC activity.

The size distribution of the nanoparticles might affect the overall PC activity. As shown in Fig. 1, the hydrothermal process produces a wide range of particles, most of which are greater than 1 micron in diameter. Studies by Chen *et al*. found that nanoparticles of uniform size favorably affected the photocatalytic activity of undoped TiO_2 (Chen *et al.* 2010). They were able to create monodisperse, mesoporous TiO_2 nanoparticles by using a hybrid technique whereby a sol gel

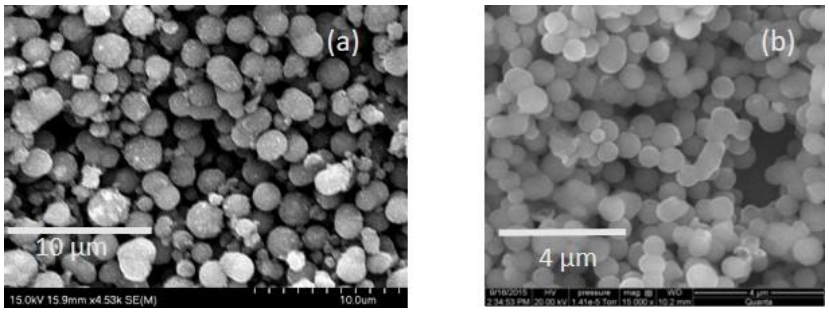

Fig. 1 SEM images of (Cu,N) TiO_2 of particles prepared using (a) the hydrothermal method and (b) the hybrid method

process was used to produce monodisperse TiO_2 nanoparticles, and then these nanoparticles were used as a template for further crystal mesoporous growth using hydrothermal processing. They discovered that the size of the particles had a significant effect on the photocatalytic activity, and the optimum size for the monodisperse nanoparticles for optimum PC activity was found to be in the neighborhood of 800 nm. It is thought that uneven sizes facilitate the recombination of electrons and holes before they can affect reduction/oxidation, thus reducing the PC efficiency (Chen *et al*. 2010).

The question naturally arises as to whether combining codoping with the abovementioned hybrid method will further increase PC activity. To that end, this paper describes the synthesis of monodisperse, codoped titania nanoparticles. The PC activity associated with them is compared to those produced by the hydrothermal technique.

2. Materials and measurement methods

Hydrothermal synthesis of the codoped titania samples is described in an earlier paper (Mathis *et al*. 2013). For example, to form (Mn,N)TiO_2, 1.55 g of a 20% $TiCl_3$ in 3% HCl solution is added to a solution consisting of 12.4 mg $Mn(CH_3COO)_2 \cdot 4H_2O$, 3.0 g urea, and 3.0 mL de-ionized water dissolved in 17.0 mL ethanol. The solution is stirred overnight and then transferred to a Teflon-lined autoclave. The autoclave is heated to 180℃ for 10 hours. Then, the material is rinsed with 500 mL de-ionized water, dried, and calcined at 550℃ for 5 hours. Nitrogen doping is accomplished by flowing ammonia over the sample in a tube furnace at 550℃ for 5 hours.

The synthesis of the porous hybrid particles followed the procedure as previously described by Chen *et al.* (2010). First, the sol gel precursor solution consisting of 2.50 g of hexadecylamine (Sigma Aldrich), 250. mL of reagent ethanol (BDH), and 1.0 mL 0.10M KCl was stirred overnight. Then, 5.7 mL of titanium tetraisopropoxide (Sigma Aldrich) was then added drop wise to the rapidly stirred solution. The resultant milky-appearing, colloidal suspension was allowed to stand overnight to allow the precipitate to settle. The precipitate was then rinsed with ethanol, centrifuged and repeated three times. The precipitate was dried at 110℃ for two hours and then transferred to a tube furnace where it was heated to 350℃ for 5 hours to drive off any remaining organic material. This step was found to be necessary as otherwise the nanoparticles will fuse together during the solvothermal step. The material was then ground into a fine powder using a mortar and pestle.

The monodisperse, titania nanoparticles produced from the first stage serve as templates for the solvothermal step. These were mixed overnight with a solution of reagent ethanol and de-ionized water to which an appropriate mole percentage of the metal acetate is added. In a typical synthesis, to achieve a 2.5 mole percent metal doping level, 1.1 g of titania is added to 14.0 mL reagent ethanol, 7.0 mL de-ionized water and 88 mg $Mn(CH_3COO)_2 \cdot 4H_2O$ (Sigma Aldrich). The solution is then transferred in an autoclave and heated for 16 hours at 160℃. Next, the material is rinsed with 500 mL de-ionized water and dried. Calcining the titania was accomplished by heating the material to 550℃ in a tube furnace under ambient air. For doping with nitrogen, the tube was then sealed and ammonia gas circulated over the sample for an additional 5 hours while the furnace temperature remained at 550℃. Calcining at 650℃ was tried since it had been reported (Wang, et al. 2013) that improved crystallinity and porosity of the templated titania could be achieved at that temperature without the attendant transition to rutile or brookite phases.

A Hitachi S4700 field emission scanning electron microscope (SEM) and an FEI Quanta 650

SEM were used to examine the microstructure of the samples. A PANalytic X-ray diffraction (XRD) spectrometer was to identify the crystalline phases present in the samples, using Cu K_α radiation.

Brunauer, Emmett, Teller (BET) analysis was used to determine the presence of mesoporosity. The samples were degassed overnight, and N_2 gas was used.

Diffuse-reflectance UV−vis spectra were collected on a Varian Cary 5000 UV−vis−NIR spectrophotometer under %R mode. The %R was then converted to absorbance units.

Photocatalytic activity was measured by monitoring the color change in a solution formed by mixing of 22 mg of the doped TiO_2 powder into 30. mL of an aqueous methylene blue solution. The mixture was stirred overnight in a dark environment to attain adsorption/desorption equilibrium. A Schoeffel 125 watt xenon arc lamp illuminated the 50 mL Pyrex reaction vessel. Ultraviolet light was filtered out by means of a 420 nm cutoff filter placed in the light path. The illuminance at the sample was 8.0×10^4 lux. Aliquots were taken at 15 minute intervals for the first half hour, then at 60 minutes, with a final aliquot taken at the 120 minute mark. The aliquots were filtered using 0.2 μm disc filters, and the filtrates' absorption was then measured with the Varian Cary 5000 spectrometer operating in absorption mode from 550 nm to 800 nm with background correction and using a water blank.

3. Results and discussion

There is a clear distinction in the size distribution between the two methods. Nearly monodisperse nanobeads were produced with the hybrid method, while the hydrothermal method produced, as before, beads with a wide range of sizes as shown in Fig. 1 and Table 1. Diameter measurements were made on a minimum of 24 nanobeads using the SEM measurement tool. The variation in size for the hybrid samples' diameters is much less than those of the hydrothermal's as shown by the smaller standard deviation.

X-ray diffraction scans show that mainly the anatase phase is present for nanobeads produced by both methods as shown in Fig. 2. A small amount of rutile is present in all the samples, with the exception (Ni,N)TiO_2. The small peak for the (Cu,N)TiO_2 sample at 2θ=33° is assigned to CuO. Consequently, it is possible that the amount of Cu present in the lattice is somewhat less than 2.5 percent. In contrast to the paper by Wang et al. (Wang *et al*. 2013), which reported that improved crystallinity occurred when hybrid titania was calcined at 650℃ while retaining the anatase phase, the template-based titania of this study, when calcined at that temperature, showed a substantial

Table 1 Size distribution of (M,N)TiO_2 beads produced by the two methods

Composition	Mean diameter (nm)	Std. deviation (nm)
(Mn,N)TiO_2 hydrothermal	1348	624
(Mn,N)TiO_2 hybrid	810	192
(Co,N)TiO_2 hydrothermal	786	396
(Co,N)TiO_2 hybrid	558	92.9
(Ni,N)TiO_2 hybrid	854	148
(Cu,N)TiO_2 hydrothermal	1673	524
(Cu,N)TiO_2 hybrid	672	120.

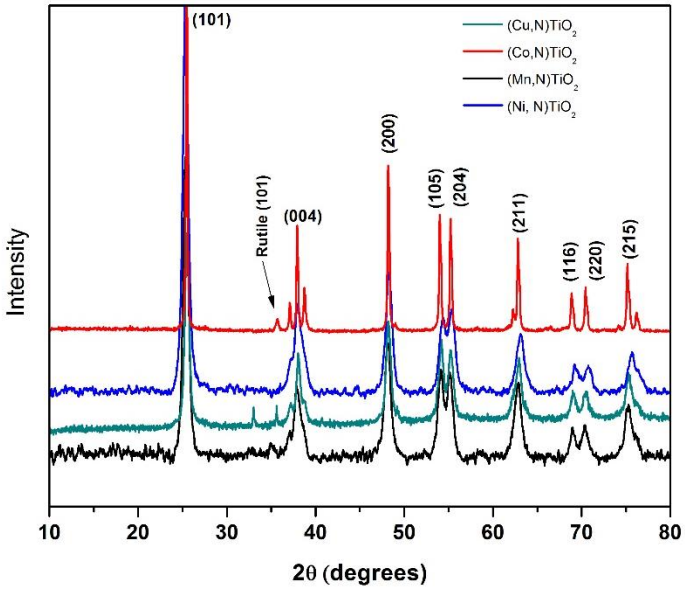

Fig. 2 XRD patterns for the codoped TiO_2 produced by the hybrid method showing the predominant anatase phase. Peaks are indexed for anatase

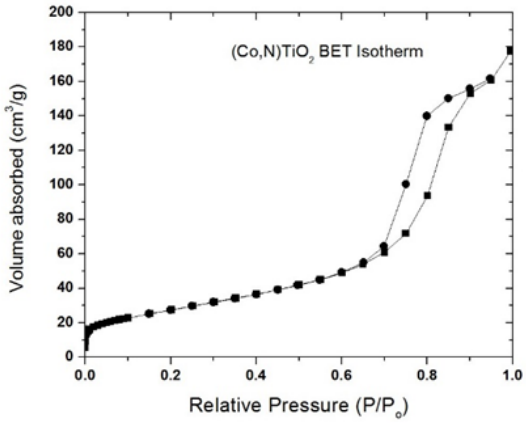

Fig. 3 BET isotherm plot of $(Co,N)TiO_2$

amount of the Brookite phase as well as the anatase. Moreover, the nickel-doped sample calcined at 650℃ contained a substantial amount of $NiTiO_3$ as shown by both the XRD scan and the "cool yellow" color of the powder, which is characteristic of nickel titanate (Albala 2010). Hence, calcining at 550℃ is close to the maximum temperature for which the anatase phase is stable.

The nanoparticles are mesoporous as shown in Fig. 3 of a typical BET isotherm plot of $(Co,N)TiO_2$ where there is a characteristic hysteresis in the adsorption-desorption process. However, macro pores are also present, which reduces the average surface area to 24 m^2/g. This is much smaller than the 86 m^2/g value for the hydrothermally-produced nanoparticles, reported in an earlier paper (Mathis *et al*. 2016) that were free of macro pores.

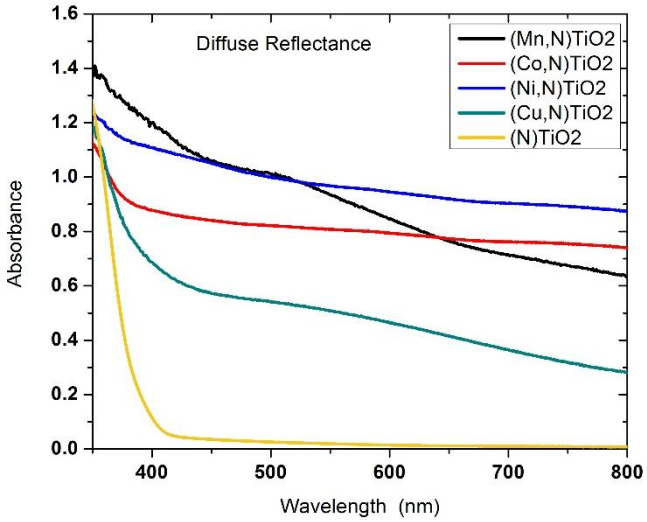

Fig. 4 Diffuse reflectance absorption measurements of codoped TiO_2 produced by the hybrid method as compared to that of N-TiO_2

Examination of the diffuse reflectance spectra of the codoped titania nanoparticles produced by the hybrid method reveals the absorption for all samples has increased dramatically and has shifted to the red as shown in Fig. 4. The absorption values are comparable to those of the earlier study (Mathis *et al*. 2013) of codoped titania nanoparticles produced the hydrothermal method. The band gaps for the codoped titania that were determined in the earlier study had a narrow range of 1.9 eV to 2.1 eV (Mathis *et al*. 2013), while the N-doped Ti had a band gap of 2.4 eV.

2.1 Photocatalytic activity

There is a clear difference in photocatalytic activity between the samples produced by the hydrothermal method and by the hybrid method. As shown in Table 2 and Fig. 5, the samples produced by the hybrid method, when exposed to the filtered light for two hours, reduced the concentration of methylene blue approximately two times more than that of the hydrothermally-produced samples. Among the samples produced by the hybrid method, the (Cu,N)TiO_2 sample had the highest activity, producing a 23 percent decrease in the concentration of methylene blue. As mentioned earlier, the percentage of Cu could be slightly lower owing to the presence of CuO as revealed by XRD. Whether this accounts for (Cu,N)TiO_2's slightly higher PC activity is uncertain since the optimum value for metal doping has not been established. As with the hydrothermal method, monodisperse (Mn,N)TiO_2 had the second-highest PC activity, with nearly a 17 percent reduction, while (Co,N)TiO_2 showed the lowest PC activity for both growth methods. As reported earlier (Mathis *et al.* 2016), codoping TiO_2 nanobeads with the same metals as in this report and produced by the hydrothermal method, had photocatalytic activities approximately 20 percent greater than of TiO_2 nanobeads doped with just nitrogen. To test whether methylene blue in solution by itself decomposed under visible-light irradiation, blank solution samples consisting of just methylene blue and de-ionized water were tested for changes in methylene blue concentration by exposing them to the light. No decay in concentration was observed.

Table 2 Percent decrease in the concentration of methylene blue after two hours of visible light exposure

	Growth Method	
Composition	Hydrothermal	Hybrid
$(Mn,N)TiO_2$	6.42	16.9
$(Co,N)TiO_2$	4.23	11.9
$(Ni,N)TiO_2$	8.72	13.7
$(Cu,N)TiO_2$	6.66	23.0

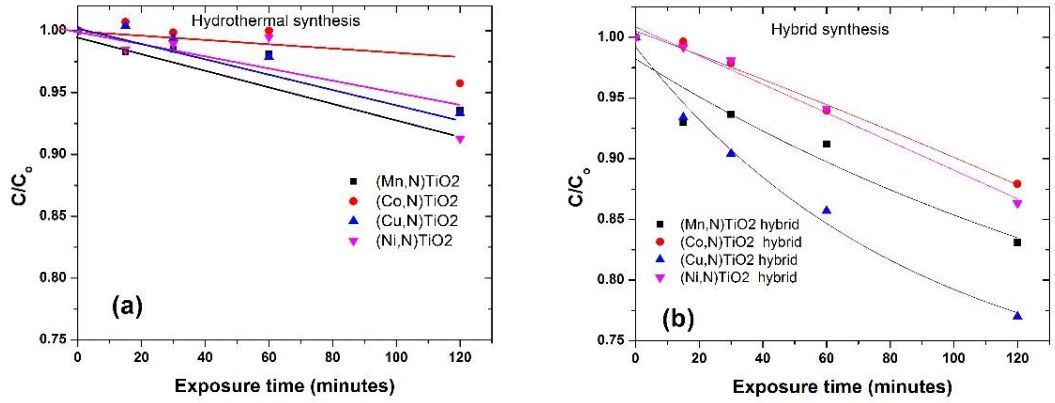

Fig. 5 Comparison between the change in methylene blue concentration caused by the exposure to visible light by nanoparticles produced by (a), the hydrothermal method and (b), the hybrid method. Lines are to guide the eye

A possible explanation for the better PC performance of the monodisperse samples is that the reactants are hindered less by the more regular arrangement of the nanobeads of the monodisperse type, whereas the more tortuous paths characteristic of particles of widely diverse size create obstacles for the reactants.

4. Conclusions

The results show that it is indeed possible to dope titania nanospheres with metals during the solvothermal growth phase of the hybrid method while maintaining mesoporous and anatase characteristics. The resulting nanospheres were mesoporous and showed a comparable increase in visible-light absorption when codoped with nitrogen as those produced using just the hydrothermal method. Moreover, the codoping process did not alter the monodisperse nature that is characteristic of the hybrid method.

The PC activity of the hybrid-synthesized nanospheres was much higher than that of the hydrothermally-produced nanospheres, with the PC activity of $(Cu,N)TiO_2$ far exceeding the others. So, it has been shown, firstly, that codoping mesoporous titania nanobeads increases the visible-light PC activity compared to undoped titania, and that, secondly, even higher PC activity is obtained when the codoped, mesoporous titania nanobeads have a narrow size distribution.

Acknowledgments

Materials synthesis work was sponsored by the U.S. Department of Energy, Office of Science, Basic Energy Sciences, Materials Sciences and Engineering Division. Characterization work was supported by Oak Ridge National Laboratory's CNMS User Facility, which is sponsored by the Scientific User Facility Division, Office of Basic Energy Sciences, U.S. Department of Energy. JM is supported by ORISE through U.S. Department of Energy-Visiting Faculty Program (VFP). MKK acknowledges the support of the U.S. Department of Energy, Office of Basic Energy Science, Chemical Sciences, Geosciences, and Biosciences Division. Thanks are due to G. E. Jellison for providing instruments for the photocatalytic measurements, and to R. A. Caruso for useful discussions. This manuscript has been authored by UT-Battelle, LLC under Contract No. DE-AC05-00OR22725 with the U.S. Department of Energy. The United States Government retains and the publisher, by accepting the article for publication, acknowledges that the United States Government retains a non-exclusive, paid-up, irrevocable, world-wide license to publish or reproduce the published form of this manuscript, or allow others to do so, for United States Government purposes. The Department of Energy will provide public access to these results of federally sponsored research in accordance with the DOE Public Access Plan (http://energy.gov/downloads/doe-public-access-plan).

References

Albala, M. (2010), Nickel Titanate, the Coolest Yellow, July 8. Accessed August 2015. http://blog.mitchalbala.com/nickel-titanate-the-coolest-yellow.

Benko, G., Skårman, B., Wallenberg, R., Hagfeldt, A., Sundstrom, V. and Yartsev, A.P. (2003), "Particle size and crystallinity dependent electron injection in fluorescein 27-sensitized", *J. Phys. Chem. B*, **107**, 1370-1375.

Bi, Z., Paranthaman, M.P., Guo, B., Unocic, R.R., Meyer III, H.M., Bridges, C.A., ... and Dai, S. (2014), "High performance Cr, N-codoped mesoporous TiO_2 microspheres for lithium-ion batteries", *J. Mater. Chem. A*, **2**, 1818-1824.

Chen, D., Cao, L., Huang, F., Imperia, P., Cheng, Y.B. and Caruso, R.A. (2010), "Synthesis of monodisperse mesoporous titania beads with controllable diameter, high surface areas, and variable pore diameters (14-23 nm)", *J. Amer. Chem. Soc.*, **132**, 4438-4444.

Dorman, J.A., Weickert, J., Reindl, J.B., Putnik, M., Wisnet, A., Noebels, M., ... and Schmidt-Mende, L. (2014), "Control of recombination pathways in TiO_2 nanowire hybrid solar cells using Sn^{4+} dopants", *J. Phys. Chem. B*, **108**(30), 16672-16679.

Li, Y., Wang, W., Qiu, X., Song, L., Meyer III, H.M., Paranthaman, M.P., Eres, G., Zhang, Z. and Gu, B. (2011), "Comparing Cr, and N only doping with (Cr, N)-codoping for enhancing visible light reactivity of TiO_2", *App. Cat B: Env.*, **110**, 148-153.

Liu, Y., Szeifert, J.M., Feckl, J.M., Mandlmeier, B., Rathousky, J., Hayden, O., ... and Bein, T. (2010), "Niobium-doped titania nanoparticles: synthesis and assembly into mesoporous films and electrical conductivity", *ACS Nano*, **4**(9), 5373-5381.

Mathis, J.E., Lieffers, J., Mitra, C., Reboredo, F.A., Bi, Z., Bridges, C.A., Kidder, M.K. and Paranthaman, M.P. (2016), "Increased photocatalytic activity of TiO_2 mesoporous microspheres from codoping with transition metals and nitrogen", *Ceramics Int.*, **42**(2), 3556-3562.

Mathis, J.E., Bi, Z., Bridges, C.A., Kidder, M.K. and Paranthaman, M.P. (2013), "Enhanced visible-light absorption of mesoporous TiO_2 by co-doping with transition-metal/nitrogen ions", *MRS Proceedings* dx.doi.org/10.1557/opl.2013.666: 1547.

Park, Y.R. and Kim, K.J. (2005), "Structural and optical properties of rutile and anatase TiO_2 thin films: effects of Co doping", *Thin Solid Film*., **484,** 34-38.

Pascoe, A.R., Chen, D., Huang, F., Duffy, N.W., Caruso, R.A. and Cheng, Y.B. (2014), "Charge transport in photoanodes constructed with mesoporous TiO_2 beads for dye-sensitized solar cells", *J. Phys. Chem. C* **118**(30), 16635-16642.

Seo, H., Baker, L.R., Hervier, A., Kim, J., Whitten, J.L. and& Somorjai, G.A. (2011), "Generation of highly n-type titanium oxide using plasma fluorine insertion", *Nano Lett.*, **11**(2), 751-756.

Thompson, T.L. and Yates, J.T. (2006), "Surface science studies of the photoactivation of TiO_2-new photochemical processes", *Chem. Rev.*, **106**, 4428-4453.

Tiwana, P., Docampo, P., Johnston, M.B., Snaith, H.J. and Herz, L.M. (2011), "Electron mobility and injection dynamics in mesoporous ZnO, SnO_2, and TiO_2 films used in dye-sensitized solar cells", *ACS Nano*, **5**(6), 5158-5166.

Wang, X., Cao, L., Chen, D. and Caruso, R.A. (2013), "Engineering of monodisperse mesoporous titania beads for photocatalytic applications", *Appl. Mater. Interfac.*, **5**, 9421-9428.

Wang, Y., Brezesinski, T., Antonietti, M. and Smarsly, B. (2009), "Ordered mesoporous Sb-, Nb-, and Ta-doped SnO_2 thin films with adjustable doping levels and high electrical conductivity", *ACS Nano*, **3**(6), 1373-1378.

Yamada, N., Hitosugi, T., Hoang, N.L.H., Furubayashi, Y., Hirose, Y., Shimada, T. and Hasegawa, T. (2007), "Fabrication of low resistivity Nb-doped TiO_2 transparent conductive polycrystalline films on glass by reactive sputtering", *Jap. J. App. Phys.*, **46**(8R), 5275.

Zhu, W., Qiu, X., Iancu, V., Chen, X.Q., Pan, H., Wang, W., ... and Stocks, G.M. (2009), "Band gap narrowing of titanium oxide semiconductors by noncompensated anion-cation codoping for enhanced visible-light photoactivity", *Phys. Rev. Lett.*, **103**, 226401.

CC